LAWOFS 2024

LATIN AMERICAN WORKSHOP ON OPTICAL FIBER SENSORS

IBERO-AMERICAN EDITION

May 20-22, 2024

Campinas, Brazil

TECHNICAL PROGRAM AND BOOK OF ABSTRACTS

TECHNICAL CO-SPONSORSHIP

IEEE

IEEE Photonics Society

REALIZATION

sbmo Sociedade Brasileira de Micro-ondas e Optoeletrônica

UNICAMP

All-fiber optomechanical cavity as a mass frequency-out sensor

Anna I. Garrigues-Navarro*, Martina Delgado-Pinar, Antonio Díez, Miguel V. Andrés
Departamento de Física Aplicada y Electromagnetismo, ICMUV, Burjassot.
*ana.i.garrigues@uv.es

***Abstract*—This research presents an optical microbalance design, based on an optical fiber ring resonator with a nested mechanical resonant cavity. Our proposal employs the optical cavity to interrogate the mechanical system. Thus, a frequency-out sensor capable of accurately measuring any small mass attached to the mechanical resonator is demonstrated. We evaluate the proposal as an all-optical microbalance for biosensor applications.**

***Index Terms*—optical fiber sensors, optomechanics, microbalance, frequency-out sensor**

I. Introduction

Sensors based on mechanical resonators have a high intrinsic interest due to the frequency encoding of the reading. In addition, optical monitoring of the sensors using optical fiber technology provides remote operation and good performance in harsh environments. Here, we investigate the use of high Q optical fiber rings to interrogate a micromechanical resonator defined by a simple short section of uncoated optical fiber. Since the mechanical vibrations are sensitive to any small mass change, the resonator defines a frequency-out microbalance with potential biosensing applications.

II. Experimental setup

A. Optical cavity characterization

Our optical ring resonator, constructed with SMF-28 fiber, uses a directional 90:10 coupler, with the 10% output arm spliced to the free input arm. A polarization controller positioned outside the cavity ensures optimal polarization alignment. We employed a narrow linewidth tunable diode laser (<100 Hz) as the light source and detected the output using a photodiode and oscilloscope (350 MHz bandwidth). The mechanical resonating cavity consisted of a small section of the fiber ring fixed at both ends to two piezoelectric pieces connected to an AC generator, as depicted in Fig. 1

When the mechanical cavity is inactive, the output of the optical ring is similar to the reflection of a Fabry-Perot interferometer, exhibing a series of transmission notches (see inset Fig. 2). Fig. 2 presents the system's characterization, including the theoretical response based on measured parameters presented in Table I.

TABLE I
Optical resonance parameters

Q factor	*FSR (fm)*	$\Delta\lambda_{3dB}$ *(fm)*	*Visibility (%)*
(1.7±0.2)·10^8	983±49	9±1	42.2±0.3

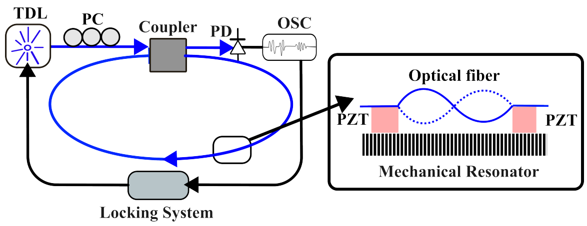

Fig. 1. *Schematics of the cavity set-up including the mechanical resonator (right). TDL: Tunable Diode Laser; PC: Polarization Controller; PD: Photodiode; OSC: Oscilloscope; MRC: Mechanical Resonating Cavity; PZT: Piezoelectric.*

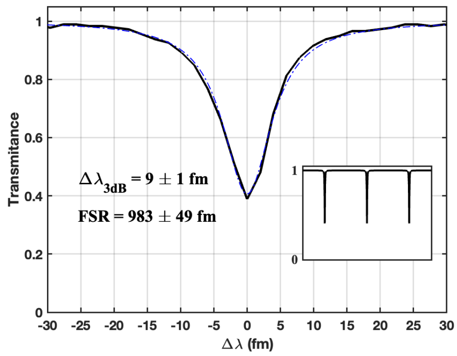

Fig. 2. *Transmission of the system with the mechanical cavity off. Inset shows a wider range of wavelength to appreciate the visibility and finesse. We show the calculated (dashed blue line) and the measured response (black solid line).*

B. Measuring method. Mechanical cavity on.

In order to operate the optical ring at a fixed working point, we implement a locking system to ensure consistent operation at half the notch amplitude, where the transmittance exhibits approximate linearity with wavelength variations. When the mechanical cavity approaches resonance, it modulates the phase of the optical ring, resulting in an oscillating transmittance at the mechanical cavity's resonance frequency.

C. Acoustic resonant cavity characterization

The resonator is defined by a section of the optical fiber with fixed ends. The flexural frequencies of resonance of a silica rod are given by [1]:

$$f_n = \frac{1}{2\pi}\sqrt{\frac{C_n E}{\rho}}\frac{a}{2L^2}, \tag{1}$$

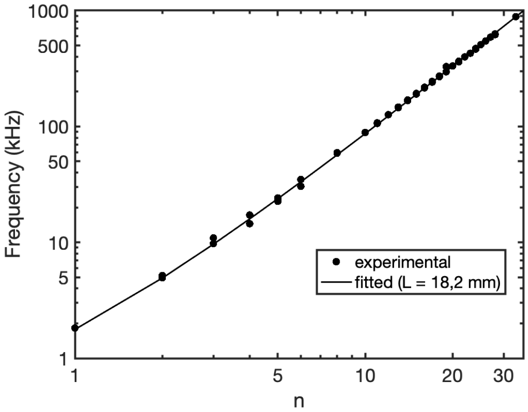

Fig. 3. *Resonance frequencies versus n, order of resonance.*

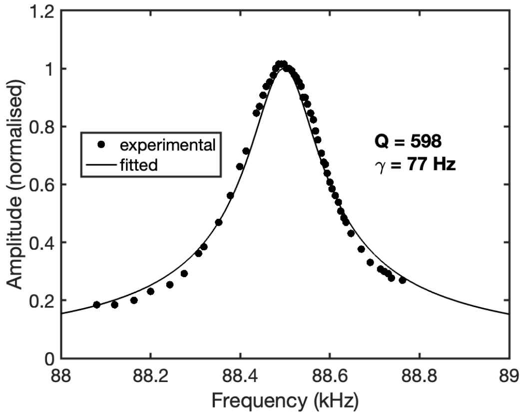

Fig. 4. *Characterization of the narrowest acoustic resonance in amplitude. Corresponds to n = 10. γ is the resonance half bandwidth.*

where E is the Young's modulus, ρ is the density, n the order of resonance and C_n constants determined by the boundary conditions.

$$C_n \approx \left[\left(n + \frac{1}{2}\right)\pi\right]^4. \quad (2)$$

III. Experimental results

The resonance frequencies obtained from our experimental measurements are depicted in Fig. 3. The length of the resonator was obtained by fitting the experimental data to Eq. 1.

The observed resonance frequencies exhibit small deviations from the fitted curve, which can be attributed to two primary effects. Firstly, the presence of two independent transversal modes of oscillation for each resonance order (n) results in a degeneracy due to the cylindrical symmetry of the resonator. However, slight asymmetries in the resonator structure lead to the splitting observed clearly in some resonances. Secondly, deviations from ideal boundary conditions, caused by irregularities in the placement of adhesive drops, introduce further deviations from the theoretical model and contribute to the observed symmetry breaking.

We also performed a close characterization for several resonance orders. We present the narrowest one in Fig. 4, with a Q factor of about 600.

IV. Sensing application

Our proposed sensor application consists of using the frequency-out characteristics to relate changes in the resonance frequency of the mechanical resonator with mass variations, as the commercial quartz mass balances do. In this framework, we aim to path the way for the transference of this kind of electronic technology into Photonics.

We carried out a theoretical evaluation of sensing performance. The quantities in which we are interested are sensitivity, resolution, detection limit, and working range [2]. The calculations were performed assuming that in a biosensor application a thin layer of molecules will be attached to the surface of the fiber increasing the radius of the resonator (we assumed that the density of this biolayer is the same as the density of the resonator). The calculated quantities are showed in Table II.

TABLE II
Optical resonance parameters

Sensitivity	***Resolution***	***Detection Limit***	***Range***
74.8 Hz/μg	7.7 Hz	103 ng	225 μg

Standard values for SMF-28 were considered. All the values were calculated for the resonance $n = 10$ since that was the narrowest measured. We considered the 5% of the resonance bandwith as the resolution. The range is estimated as the mass variation that corresponds to a frequency shift equivalent to the FSR between acoustic resonances.

V. Conclusion

In conclusion, our research presents a novel approach utilizing mechanical resonators for sensing applications.

While the current results may not be immediately applicable to practical biosensing, they highlight promising potential. Further improvements can be obtained tapering the optical fiber down to a few microns and working with higher resonant frequencies.

Acknowledgment

This research was funded by the Ministerio de Ciencia e Innovación and co-funded by the European Regional Development Fund, Ref. TED2021-130200B-I00, the European Commission, Ref. H2020-MSCARISE-2019-872049 and the Generalitat Valenciana, Ref. CIPROM/2022/030. A.I. Garrigues Navarro thanks OPTICA (formerly OSA) for her scholarship OPTICA Women Scholars Programme 2022 Class.

References

[1] J. M. Seelig and I. Hoppmann, W. H., "Normal mode vibrations of systems of elastically connected parallel bars," vol. 36, no. 1, pp. 93–99.

[2] I. M. White and X. Fan, "On the performance quantification of resonant refractive index sensors," vol. 16, no. 2, p. 1020.